NUCLEAR THEORY, Vol. 42 (2025)
eds. M. Gaidarov, N. Minkov, Heron Press, Sofia

Symplectic Symmetry Approach to Clustering in Atomic Nuclei: The Case of ^{20}Ne

H.G. Ganev[1,2]

[1]Joint Institute for Nuclear Research, Dubna, Russia
[2]Institute of Mechanics, Bulgarian Academy of Sciences, Sofia, Bulgaria

Abstract. Symplectic symmetry approach to clustering (SSAC) with the essential group structure $Sp(6,R)_R \otimes Sp(6,R)_C \otimes O(A-2) \subset Sp(6(A-1),R)$ is applied to the microscopic description of the lowest $K^\pi = 0_1^+$, $K^\pi = 0_1^-$, and $K^\pi = 0_2^+$ rotational bands in the classical two-cluster α + ^{16}O $\rightarrow$ ^{20}Ne nuclear system. The latter consists of two scalar $SU(3)$ clusters, so in this particular case the more complete cluster dynamics within the SSAC is reduced to a pure intercluster dynamics of the R-subsystem only. A good description for the excitation energies of these three bands, as well as for the experimentally known $B(E2)$ transition probabilities between the states of the ground band without the use of an effective charge, is obtained. For this purpose a simple vertical-mixing term of algebraic nature is added to the dynamical symmetry Hamiltonian, which mixes different irreducible representations from the so-called stretched $SU(3)$ states associated with the relative-motion cluster excitations.

1 Introduction

Clustering is a well established phenomenon in light nuclei [1–4]. In nuclear physics, most cluster states involve the α particle. The α cluster structure is primarily found for nuclei near $N = Z$, recognized early in the nuclear structure theory [5]. Different models of clustering in atomic nuclei have been proposed (see, e.g., [3, 4, 6–9]). The simplest variant is provided by the large class of two-cluster models.

As other nuclear structure models, the various cluster models roughly can be divided into two groups − microscopic and phenomenological models. The main characteristic that distinguishes between the two groups is provided by the Pauli principle. In microscopic models of nuclear structure, the nuclear states are described by antisymmetric many-nucleon wave functions and the Pauli principle is fully respected. Then the relative motion of the clusters is described by the wave functions of the many-particle Hilbert subspace spanned by the Pauli-allowed states. The interaction in the microscopic cluster models, however, can be either of phenomenological or modern high-precision realistic type inspired from the QCD. In the present work we use a simple phenomenological interaction of algebraic nature.

The crucial role of the Pauli principle in the models of nuclear structure has recently been shown in [10]. It turns out that it is not very easy to account for the Pauli principle within the framework of different cluster models. The methods to obtain antisymmetric states are often quite involved. It is most readily taken into account within the algebraic models of nuclear structure, in which all model observables (e.g., Hamiltonian and transition operators) are expressed in terms of dynamical groups and spectrum-generating algebras (SGA) [11]. There are different algebraic cluster models, among which we mention the algebraic cluster model (ACM) [12–15], the nuclear vibron model (NVM) [16–20], the semimicroscopic algebraic cluster model (SACM) [21,22], the semimicroscopic algebraic quartet model (SAQM) [23].

Recently, a fully algebraic microscopic symplectic symmetry approach to clustering (SSAC) in the atomic nuclei has been proposed for the two- [24] and the general multicluster nuclear systems [25], in which the Pauli principle is fully satisfied. It starts with $Sp(6(A-1),R)$ group, which is the dynamical group of the whole many-particle nuclear system and contains various nuclear excitations – collective, single particle, cluster, etc. A certain type of nuclear excitations can be isolated by reducing $Sp(6(A-1),R)$ in different way. The cluster physics in the two-cluster nuclear case is represented by the following group structure $Sp(6,R)_R \otimes Sp(6,R)_C \otimes O(A-2) \subset Sp(6(A-1),R)$, in which $Sp(6,R)_R \otimes Sp(6,R)_C$ describes both the inter and internal cluster excitations on the same footing, while the group $O(A-2)$ allows to ensure the proper, physical permutational symmetry of the nuclear cluster system.

The SSAC has been applied to the description of low-lying rotational bands of positive- and negative-parity states in the two-cluster ^{20}Ne + $\alpha \rightarrow {}^{24}$Mg [24] and the four α-cluster [25] nuclear systems, respectively. The purpose of the present work is to apply the SSAC to the classical two-cluster α + ^{16}O $\rightarrow {}^{20}$Ne nuclear system. In particular, we consider the microscopic description of the lowest three well-known experimentally established $K^\pi = 0^+_1$, $K^\pi = 0^-_1$, and $K^\pi = 0^+_2$ cluster bands in ^{20}Ne.

The structure of the low-lying collective states in ^{20}Ne has been studied in different microscopic shell-model algebraic approaches. From the early works (see a review paper by Harvey [26]), we mention that of Akiyama, Arima, and Sebe [27], in which the shell-model calculations have been performed for some ds-shell nuclei using a phenomenological effective interaction of the central Yukawa type. It has been shown that the $SU(3)$ multiplets $(8,0)$ and $(6,1)$, with corresponding space symmetry $[4]$ and $[31]$, exhaust up to 95% of the structure of the ground state band. The dominant $SU(3)$ component is given by the $(8,0)$ multiplet and is about $80-90\%$ for different angular momentum states within the ground band. Microscopic shell-model calculations of the structure of ground band and first few resonance excited bands in ^{20}Ne have been performed within the framework of the microscopic $Sp(6,R)$ model of collective motion by using a simple phenomenological interactions of algebraic form [28,29]. These calculations showed that the dominant contribution to the microscopic structure of the

ground band states is provided by the so-called stretched states which are $SU(3)$ states of the type $(\lambda_0 + 2n, \mu_0)$ with $n = 0, 1, 2, \ldots$ [30]. In particular, 90% of the ^{20}Ne ground state comes from the $(8, 0)$, $(10, 0)$ and $(12, 0)$ stretched states [28]. The results of [28] showed an excessive collectivity compared to the experimental data. Finally, *ab initio* large-scale multi-shell calculations within the framework of the symmetry-adapted no-core shell model [31], in which the $U(3) \otimes SU(2)_{S_p} \otimes SU(2)_{S_n}$ coupled basis is used with no *a priori* symmetry constraints, have been applied to the description of low-energy nuclear structure in some light nuclei, including ^{20}Ne, using various QCD-inspired realistic interactions. Unfortunately, only the ground band in ^{20}Ne was considered with the intraband $B(E2)$ transition strengths up to $L = 4$, in which the structure is dominated by a single deformed shape that results from the leading $SU(3)$ irrep $(8, 0)$.

Despite of the well pronounced collectivity of the observed rotational bands, actually ^{20}Ne exhibits a complicated character revealed by the more detailed shell-model culculations. Indeed, the microscopic calculations of Ref. [32], exploring the competition between the quadrupole and L-paring coupling schemes in the ds nuclear shell, indicate that ^{20}Ne lies very close to the critical point between the $SU(3)$ and $O(6)$ shell-model limits. Thus, this nucleus serves as a good example that can be used to test the different collective models of nuclear structure.

2 Theoretical framework

In order to avoid the problem of the center-of-mass motion we consider the $m = A-1$ translationally invariant relative Jacobi coordinates q_{is} of the whole nuclear system. One linear combination of the $(A-1)$ Jacobi vectors, denote it by $\{\mathbf{q}^R\}$, will describe the intercluster motion of the two clusters. The remaining $(A-2)$ Jacobi vectors are then related to the intrinsic structure of the two clusters. The SSAC in atomic nuclei for two-cluster nuclear systems, i.e. $A = A_1 + A_2$, is defined by the following reduction chain [24]:

$$
\begin{array}{ccccccccc}
Sp(6(A-1),R) & & & & & & & & \\
\supset & Sp(6,R)_R & \otimes & Sp(6(A_1-1),R) & \otimes & Sp(6(A_2-1),R) & & & \\
\supset & Sp(6,R)_R & \otimes & Sp(6,R)_C & \otimes & O(A-2) & & & \\
 & \langle\sigma^R\rangle & & \langle\sigma^C\rangle & & & & & \\
\supset & U_R(3) & \otimes & U_C(3) & \supset & U(3) & \supset & SO(3), & \\
 & [E_1^R,0,0] & & [E_1^C,E_2^C,E_3^C] & & [E_1,E_2,E_3] & \kappa & L\,, &
\end{array}
\tag{1}
$$

where $Sp(6,R)_C$ and $O(A-2)$ denote the corresponding direct-product groups: $Sp(6,R)_C \equiv Sp(6,R)_{C_1} \otimes Sp(6,R)_{C_2}$ and $O(A-2) \equiv O(A_1-1) \otimes O(A_2-1)$, related to the subspaces spanned by the sets $q_{C_1} = (q_1, \ldots, q_{A_1-1})$ and $q_{C_2} = (q_1, \ldots, q_{A_2-1})$ of the Jacobi coordinates of the two clusters. The essential dynamics within the SSAC is governed by the group structure $Sp(6,R)_R \otimes Sp(6,R)_C$, where $Sp(6,R)_R$ describes the intercluster excitations, whereas

$Sp(6,R)_C$ is associated with the internal excitations of the clusters. In this respect we note that the group $Sp(6,R)_C$ is also of physical significance, since for the general case of nonscalar $U_C(3)$ internal structures it indicates that many cluster excitations play an important role in the more complex cluster dynamics. Note also that the $Sp(6,R)_C$ representations are infinite-dimensional, i.e. they include infinite number of $U_C(3)$ multiplets. In practical applications one needs to consider only one or a few (lowest) $U_C(3)$ representations coupled to the large variety of the relative motions contained in the respective $Sp(6,R)_R$ representations, the latter also truncated up to a certain energy. Otherwise, especially when the excited $U_C(3)$ multiplets are included, the model space becomes very quickly too large and the well-known shell-model explosion problem arises.

From another side, the proper permutational symmetry in the SSAC is ensured via the orthogonal group $O(A-2) \equiv O(A_1-1) \otimes O(A_2-1)$ by considering the reductions $O(A_\alpha - 1) \supset S_{A_\alpha}$ with $\alpha = 1, 2$, i.e.

$$\begin{array}{ccc} O(A_1-1) & \otimes & O(A_2-1) \\ \omega_1 & & \omega_2 \\ \cup\, \delta_1 & & \cup\, \delta_2 \\ S_{A_1} & \otimes & S_{A_2} \\ f_1 & & f_2 \end{array} \qquad (2)$$

where $\omega_\alpha = (\omega_1^\alpha, \omega_2^\alpha, \omega_3^\alpha)$ denote the irreducible representations of the corresponding $O(A_\alpha - 1)$ group, related to the specific microscopic shell-model structure of the two-cluster nuclear system. Particularly, all $O(A_\alpha - 1)$ irreducible representations that contain an S_{A_α} permutational symmetry f_α of the type $[4^{k_4}, 3^{k_3}, 2^{k_2}, 1^{k_1}]$ (referred further as a physical permutational symmetry) are Pauli-allowed and retained in the shell-model spaces of two clusters. For some permutational symmetries f_α a multiplicity index δ_α is required. The Pauli-allowed $O(A_\alpha - 1)$ irreps by their dual representations determine the Pauli-allowed bandhead structures (i.e., corresponding lowest-grade $U_{C_\alpha}(3)$ irreps) of the $Sp(6,R)_{C_\alpha}$ groups in the direct-product group $Sp(6,R)_C$. This provides us with a set of Pauli-allowed $SU_{C_\alpha}(3)$ shell-model irreps for each major shell, arranged by their underlying physical permutational symmetry. The proper permutational symmetry between the clusters within the whole two-cluster nuclear system, in turn, is obtained by taking the outer product $f_1 \otimes f_2$ of these S_{A_α} irreps.

Introducing the standard creation and annihilation operators of three-dimensional harmonic oscillator quanta

$$b_i^{\dagger R} = \sqrt{\frac{\mu\omega_R}{2\hbar}}\Big(q_i^R - \frac{i}{\mu\omega_R}p_i^R\Big), \qquad b_i^R = \sqrt{\frac{\mu\omega_R}{2\hbar}}\Big(q_i^R + \frac{i}{\mu\omega_R}p_i^R\Big), \qquad (3)$$

the group of intercluster excitations $Sp(6,R)_R$ can be represented by means of the following set of generators

$$F^R_{ij} = b^{\dagger R}_i b^{\dagger R}_j, \quad G^R_{ij} = b^R_i b^R_j, \tag{4}$$

$$A^R_{ij} = \frac{1}{2}\Big(b^{\dagger R}_i b^R_j + b^R_j b^{\dagger R}_i\Big), \tag{5}$$

i.e. $Sp(6,R)_R \equiv \{F^R_{ij}, G^R_{ij}, A^R_{ij}\}$ [24]. In Eq. (3) $\mu = (\frac{A_1 A_2}{A_1 + A_2})M$ is the reduced mass and we chose $\omega_R = (\frac{A_1 + A_2}{A_1 A_2})\omega$, so that for the oscillator length parameter we obtain $b_0 = \sqrt{\hbar/(\mu\omega_R)} = \sqrt{\hbar/(M\omega)}$. As can be seen, the operators (4) create or annihilate a pair of oscillator quanta, whereas the operators (5) preserve the number of quanta and generate the subgroup $U_R(3) \subset Sp(6,R)_R$. In this way, the $Sp(6,R)_R$ generators of intercluster excitations can change the number of oscillator quanta by either 0 or 2. Thus, acting on the ground state by the $Sp(6,R)_R$ generators one can produce the positive-parity $SU(3)$ cluster-model states of even oscillator quanta only. The negative-parity cluster-model states, in turn, consist of odd number of oscillator quanta and are associated with the $SU(3)$ basis states of the odd irreps of the group $Sp(6,R)_R$.

Similarly one obtains the oscillator realizations for the dynamical group of collective (internal cluster or major shell) excitations of the two clusters

$$Sp(6,R)_C \equiv \Big\{F^C_{ij} = \sum_{s=1}^{A-2} b^\dagger_{is} b^\dagger_{js},\ G^C_{ij} = \sum_{s=1}^{A-2} b_{is} b_{js},\ A^C_{ij} = \frac{1}{2}\sum_{s=1}^{A-2}(b^\dagger_{is} b_{js} + b_{js} b^\dagger_{is})\Big\}$$

in terms of the harmonic oscillator creation and annihilation operators

$$b^\dagger_{is} = \sqrt{\frac{M\omega}{2\hbar}}\Big(q_{is} - \frac{i}{M\omega}p_{is}\Big), \qquad b_{is} = \sqrt{\frac{M\omega}{2\hbar}}\Big(q_{is} + \frac{i}{M\omega}p_{is}\Big), \tag{6}$$

where $i,j = 1,2,3$, $s = 1,2,\ldots,A-2$ and M is the nucleon mass [24]. Actually, this realization of the $Sp(6,R)_C \equiv Sp(6,R)_{C_1} \otimes Sp(6,R)_{C_2}$ group corresponds to the case when its $K_1 X_{C_1} + K_2 X_{C_2}$ generators (with $X_{C_1} \in Sp(6,R)_{C_1}$ and $X_{C_2} \in Sp(6,R)_{C_2}$) are taken in the form $X_{C_1} + X_{C_2}$, i.e. when $K_1 = K_2 = 1$. This particular case corresponds to the reduction $Sp(6,R)_{C_1} \otimes Sp(6,R)_{C_2} \supset Sp(6,R)_{C_1+C_2}$. If needed, one can consider the symplectic groups related separately to each cluster, i.e.

$$Sp(6,R)_{C_\alpha} \equiv \Big\{F^{C_\alpha}_{ij} = \sum_{s=1}^{A_\alpha - 1} b^\dagger_{is} b^\dagger_{js}\,, G^{C_\alpha}_{ij} = \sum_{s=1}^{A_\alpha - 1} b_{is} b_{js}\,, A^{C_\alpha}_{ij} = \frac{1}{2}\sum_{s=1}^{A_\alpha - 1}(b^\dagger_{is} b_{js} + b_{js} b^\dagger_{is})\Big\}$$

with $\alpha = 1,2$.

The symplectic basis states of the R- or C-subsystem are determined by the $Sp(6,R)_\alpha$ ($\alpha = R, C$) lowest-weight state $|\sigma^\alpha\rangle$, defined by [24,25]:

$$\begin{aligned} G^\alpha_{ij}|\sigma^\alpha\rangle &= 0, \\ A^\alpha_{ij}|\sigma^\alpha\rangle &= 0, \qquad i<j \\ A^\alpha_{ii}|\sigma^\alpha\rangle &= \left(\sigma^\alpha_i + \frac{m_\alpha}{2}\right)|\sigma^\alpha\rangle, \end{aligned} \tag{7}$$

and are classified by the following reduction chain

$$\begin{array}{ccc} Sp(6,R)_\alpha & \supset & U_\alpha(3). \\ \langle\sigma^\alpha\rangle & n_\alpha\rho_\alpha & [E^\alpha_1, E^\alpha_2, E^\alpha_3]_3 \end{array} \tag{8}$$

For the R-subsystem $n_R = \rho_R = m_R = 1$ and the allowed $U_R(3)$ irreps are only fully symmetric, i.e. of the type $[E^R, 0, 0]_3$. Similarly, for the C-subsystem $m_C = A-2$ and the $U_C(3)$ irreps are of general type $[E^C_1, E^C_2, E^C_3]_3$ for $A > 3$. The $Sp(6,R)_\alpha$ basis states can then be represented in the following coupled form [24,25]:

$$|\Psi(\sigma^\alpha n_\alpha \rho_\alpha E^\alpha \eta_\alpha)\rangle = [P^{(n_\alpha)}(F^\alpha) \times |\sigma^\alpha\rangle]^{\rho_\alpha E^\alpha}_{\eta_\alpha}, \tag{9}$$

where $E^\alpha = [E^\alpha_1, E^\alpha_2, E^\alpha_3]_3$ denotes the coupled $U_\alpha(3)$ irrep and ρ_α is a multiplicity label of its appearance in the product $n \otimes \sigma^\alpha$ with $n^\alpha = [n^\alpha_1, n^\alpha_2, n^\alpha_3]_3$ and $\sigma^\alpha = [\sigma^\alpha_1, \sigma^\alpha_2, \sigma^\alpha_3]_3$. Finally, the symbol η_α labels basis states of the group $U_\alpha(3)$. The basis along the reduction chain (1) can therefore be written in the form [24,25]:

$$|\Gamma; [E_R, 0, 0]_3, [E^C_1, E^C_2, E^C_3]_3; [E_1, E_2, E_3]_3; \kappa L\rangle, \tag{10}$$

where $[E_R, 0, 0]_3$, $[E^C_1, E^C_2, E^C_3]_3$, $[E_1, E_2, E_3]_3$, and L denote the irreducible representations of the $U_R(3)$, $U_C(3)$, $U(3)$, and $SO(3)$ groups, respectively. The symbol Γ labels the set of remaining quantum numbers of other subgroups in (1), and κ is a multiplicity label in the reduction $U(3) \supset SO(3)$. Using the standard Elliott's notations $(\lambda_R, \mu_R) = (E_R, 0)$, $(\lambda_C = E^C_1 - E^C_2, \mu_C = E^C_2 - E^C_3)$, and $(\lambda = E_1 - E_2, \mu = E_2 - E_3)$ for the various $SU(3)$ subgroups and the relation $N = (E_1 + E_2 + E_3) + 3(A-1)/2$ for the number of oscillator quanta (including the zero-point motion), the basis (10) can alternatively be presented as

$$|\Gamma N; (E_R, 0), (\lambda_C, \mu_C); (\lambda, \mu); \kappa L\rangle, \tag{11}$$

which turns to be more convenient and will be used in what follows. The matrix elements of different physical operators then can be represented in this basis in terms of the $SU(3)$ coupling and recoupling coefficients. The required computational technique for performing a realistic microscopic calculations is shortly presented in Ref. [24].

3 Application

The intrinsic structure of the closed-shell ^{16}O and α clusters of the ^{20}Ne nuclear system are determined by the $SU(3)$ scalar irreducible representation $(\lambda_C, \mu_C) = (0,0)$. In this case the more complete cluster dynamics within the SSAC, governed by $Sp(6,R)_R \otimes Sp(6,R)_C \subset Sp(6(A-1),R)$, is reduced to the R-subsystem dynamics. The C-subsystem does not contribute to the excitation energies and $B(E2)$ transition probabilities between the corresponding cluster states. It is well known that the leading $SU(3)$ representation for ^{20}Ne is $(8,0)$, which is chosen as a banhead of the $Sp(6,R)_R$ collective irreducible space (see Table 1) relevant to the positive-parity states of the ground $K^\pi = 0^+_1$ and first excited $K^\pi = 0^+_2$ cluster bands in ^{20}Ne. But since the relevant $SU_R(3)$ basis states in the two-cluster ^{16}O + $\alpha \rightarrow$ ^{20}Ne nuclear system are built up only by a single relative-motion Jacobi vector $\mathbf{q}^R$, only the fully symmetric $SU_R(3)$ irreps, given in red in Table 1, are Pauli permissible. The lowest-grade $SU_R(3)$ irreducible representation $(\lambda_R, 0) = (8,0)$ of the $Sp(6,R)_R$ irreducible collective space $0p-0h$ $(8,0)$ is determined by the Wildermuth condition [1] which requires for the minimum Pauli allowed number of oscillator quanta $E_R = 8$ of the intercluster excitations.

Table 1. $SU_R(3)$ basis states (λ,μ) of the $Sp(6,R)_R$ irrep $0p-0h$ $(8,0)$, relevant to the lowest positive-parity states in ^{20}Ne. The multiple appearance of $SU(3)$ multiplets is denoted by ϱ. But since the $SU_R(3)$ basis states in the two-cluster ^{16}O + $\alpha \rightarrow$ ^{20}Ne nuclear system are built up only by a single relative-motion Jacobi vector $\mathbf{q}^R$, only the fully symmetric $SU_R(3)$ irreducible representations given in red are Pauli-allowed.

E_R	$\hbar\omega$	$SU(3)$ $IR's$ $\varrho(\lambda,\mu)$
$\vdots$	$\vdots$	$\ldots$
12	4	$(12,0), (10,1), 2(8,2), (6,3), (7,1), (4,4), (6,0)$
10	2	$(10,0), (8,1), (6,2)$
8	0	$(8,0)$

For the lowest $K^\pi = 0^-_1$ negative-parity cluster band in ^{20}Ne, often considered as a partner band to the ground band, we choose the $1p-1h$ $(9,0)$ irreducible collective space of $Sp(6,R)_R$, given in Table 2.

In the present application, we use the following model Hamiltonian

$$H = H_{DS} + H_{vmix}, \tag{12}$$

where the dynamical symmetry Hamiltonian

$$\begin{aligned} H_{DS} =& \xi C_2[Sp(6,R)_R] + BC_2[SU(3)] \\ &+ C(C_2[SU(3)])^2 + \frac{1}{2\mathcal{J}} C_2[SO(3)], \end{aligned} \tag{13}$$

Table 2. $SU_R(3)$ basis states (λ,μ) of the $Sp(6,R)_R$ irrep $1p-1h$ $(9,0)$, relevant to the lowest negative-parity states in ^{20}Ne. The multiple appearance of $SU(3)$ multiplets is denoted by ϱ. But since the $SU_R(3)$ basis states in the two-cluster ^{16}O + $\alpha \rightarrow$ ^{20}Ne nuclear system are built up only by a single relative-motion Jacobi vector $\mathbf{q}^R$, only the fully symmetric $SU_R(3)$ irreducible representations given in red are Pauli-allowed

E_R	$\hbar\omega$	$SU(3)$ $IR's$ $\varrho(\lambda,\mu)$
$\vdots$	$\vdots$	...
13	5	$(13,0),(11,1),2(9,2),(7,3),(8,1),(5,4),(7,0)$
11	3	$(11,0),(9,1),(7,2)$
9	1	$(9,0)$

is expressed solely by means of the Casimir operators of the $Sp(6,R)_R$, $SU(3)$, and $SO(3)$ subgroups in the chain (1). The first three terms split in energy different $Sp(6,R)_R$ and $SU(3)$ representations, respectively. Their eigenvalues are given by the following expressions [33]:

$$\langle C_2[SU(3)]\rangle = \frac{2}{3}(\lambda^2+\mu^2+\lambda\mu+3\lambda+3\mu), \tag{14}$$

$$\langle C_2[Sp(6,R)_R]\rangle = \sum_{i=1}^{3}\sigma_i(\sigma_i+8-2i). \tag{15}$$

Additionally, to take into account different moment of inertia experimentally observed for various cluster bands, we use the following energy- and spin-dependent moments of inertia $\mathcal{J}=\mathcal{J}_0(1+\alpha_i E_i+\beta L)$. Such energy- and/or spin-dependent moments of inertia are often used in the literature (see, e.g., [34–36]). The Hamiltonian (13) acts within the irreducible collective spaces spanned only by the corresponding $Sp(6,R)_R$ bandheads (see, e.g., the lowest-grade $SU(3)$ irreps of Tables 1 and 2 given at the bottom), which can be considered as trivially obtained truncated or *effective* shell-model subspaces. Finally, the last term in Eq. (12)

$$H_{vmix} = v_{mix}\Big(A_2^R\cdot F_2^R + h.c.\Big), \tag{16}$$

introduces a vertical mixing of different $SU_R(3)$ multiplets within the corresponding $Sp(6,R)_R$ irreducible collective subspaces.

In Figure 1, we show the results of the diagonalization of the model Hamiltonian (12) for the excitation energies of the three lowest $K^\pi=0_1^+$, $K^\pi=0_2^+$, and $K^\pi=0_1^-$ cluster bands in ^{20}Ne, compared with the experimental data [37]. The values of the fitted model parameters are as follows: $\xi=0.17$, $B=-1.327$, $C=0.0033$, $v_{mix}=-0.003$ (in MeV), $\mathcal{J}_0=1.98$ (in MeV^{-1}), $\beta=0.034$, and $\alpha_{0_1^-}=0.069$. In addition, the ^{16}O + α threshold energy is also shown in

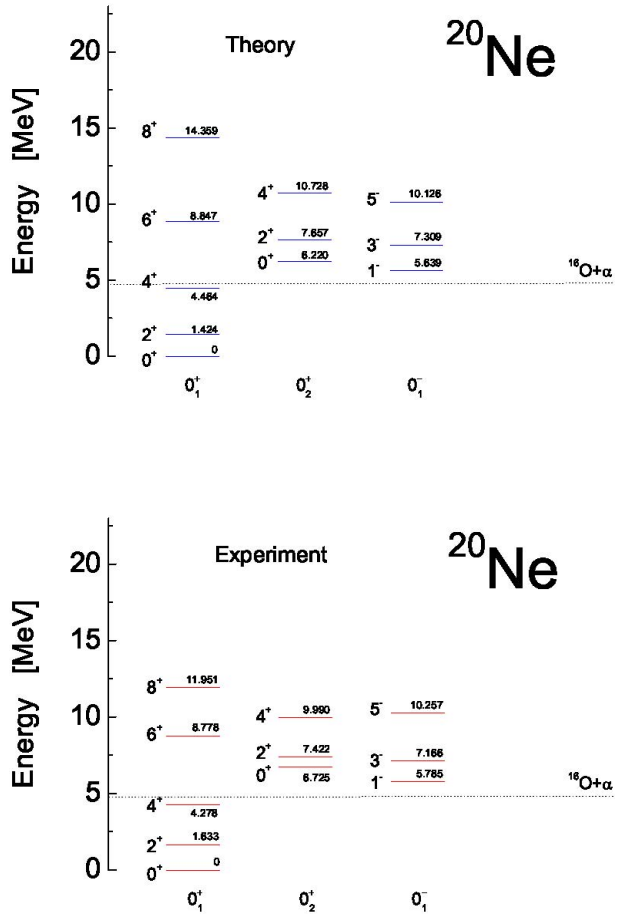

Figure 1. Theoretical and experimental [37] excitation energies of the lowest $K^\pi = 0_1^+$, $K^\pi = 0_2^+$, and $K^\pi = 0_1^-$ cluster bands in ^{20}Ne. The corresponding ^{16}O + α threshold energy is also shown for completeness.

Figure 1. From the figure one sees that the structure of three considered bands is well described.

In Figure 2, we show the intraband $B(E2)$ transition strengths in Weisskopf units between the states of the $K^\pi = 0_1^+$ and $K^\pi = 0_1^-$ bands in ^{20}Ne, compared with the available experimental data [37]. As $E2$ transition operators we use [24]:

$$T^{E2}_{2M} = \sqrt{\frac{5}{16\pi}}\left[e_{eff}Q^R_{2M} + e_{eff}\left(\frac{Z-1}{A-2}\right)Q^C_{2M}\right], \tag{17}$$

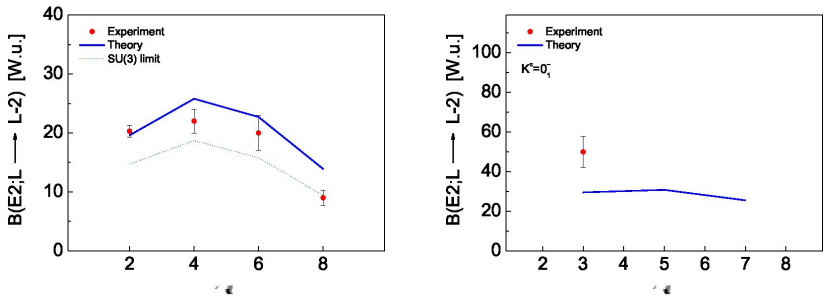

Figure 2. Comparison of the experimental [37] and theoretical intraband $B(E2)$ values in Weisskopf units between the states of the $K^\pi = 0^+_1$ and $K^\pi = 0^-_1$ bands in ^{20}Ne. For comparison, the SSAC theoretical predictions in its $SU(3)$ limit for the ground band are given as well. No effective charge is used.

where $Q^R_{2M} = \sqrt{3}\Big[A^R_{2M} + \frac{1}{2}\Big(F^R_{2M} + G^R_{2M}\Big)\Big]$ and $Q^C_{2M} = \sqrt{3}\Big[A^C_{2M} + \frac{1}{2}\Big(F^C_{2M} + G^C_{2M}\Big)\Big]$ are the quadrupole generators of the symplectic groups $Sp(6,R)_R$ and $Sp(6,R)_C$, respectively. Recall that for two-cluster α + ^{16}O $\rightarrow$ ^{20}Ne nuclear system the intrinsic quadrupole operators Q^C_{2M} do not contribute to the $B(E2)$ transition strengths. The calculations are performed without the use of an effective charge, i.e. $e_{eff} = e$. For comparison, in Figure 2 the theoretical results for the ground band in the $SU(3)$ limit are also shown, which underestimate the experimental values. A small $SU_R(3)$ admixture from the higher cluster configurations allows to reach the experimental values (cf. Figure 3). From the figure one sees that although the description of the $B(E2)$ transition strengths is not perfect, but the trend is well described. The theoretical values slightly overestimate the experiment for the higher angular momenta, especially for $L = 8$. For the interband $B(E2; 0^+_2 \rightarrow 2^+_1)$ and $B(E2; 4^+_2 \rightarrow 2^+_1)$ transition probabilities we obtain 0.63 and 0.95 W.u., which significantly underestimate the experimental values 3.6 and 5.8 W.u., respectively. For $B(E2; 3^-_1 \rightarrow 1^-_1)$ we get 29.5 W.u., to be compared with the experimental value 50(8) W.u., which is in a reasonable agreement.

Actually ^{20}Ne possesses a complicated structure and it was shown to lie very close to the critical point between the $SU(3)$ and $O(6)$ shell-model limits of the ds shell [32]. The $O(6)$ Casimir operator in the shell-model calculations in [32], associated with the L-pairing in the ds shell, actually introduces a horizontal mixing of different $SU(3)$ multiplets within the ds shell. The underestimated interband $B(E2)$ transition strengths point out that the description can be improved in a more sophisticated microscopic calculations within the present SSAC, in which both the vertical and horizontal mixings of different $SU(3)$ irreducible representations are taken into account, in a manner similar to that given in Ref. [38] within a microscopic shell-model version of the Bohr-Mottelson

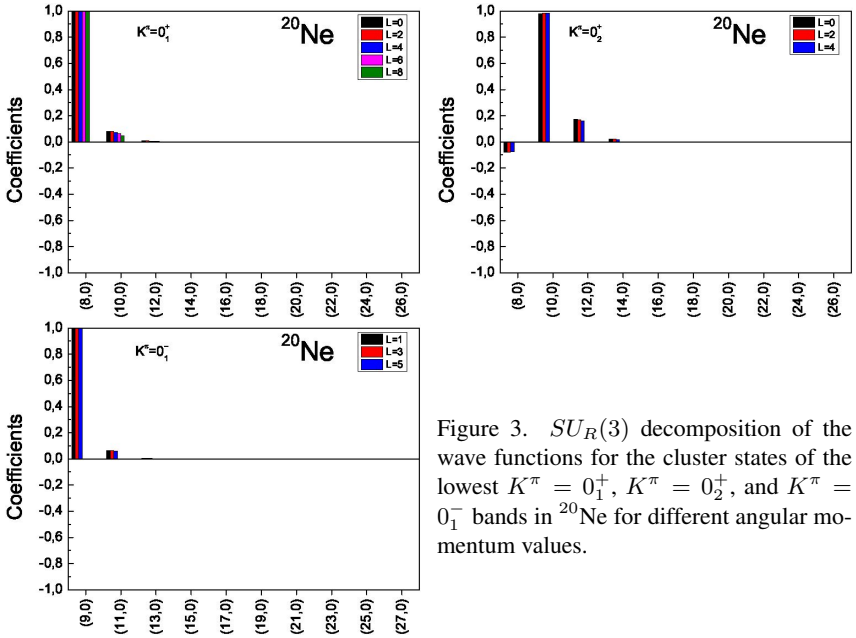

Figure 3. $SU_R(3)$ decomposition of the wave functions for the cluster states of the lowest $K^\pi = 0_1^+$, $K^\pi = 0_2^+$, and $K^\pi = 0_1^-$ bands in ^{20}Ne for different angular momentum values.

collective model. Pauli-allowed $0\hbar\omega$ $SU(3)$ irreps for ^{20}Ne in the spin-isospin occupation scheme are provided by the set: $(8,0)$, $(4,2)$, $(0,4)$, and $(2,0)$. For the two-cluster α + ^{16}O $\rightarrow$ ^{20}Ne nuclear system within the SSAC, this set of $0\hbar\omega$ $SU(3)$ multiplets belongs to different $Sp(6,R)_R$ irreducible many-particle subspaces of the Hilbert space of ^{20}Ne, built up on these $SU_R(3)$ multiplets which represent the corresponding symplectic bandheads. Thus, to mix different $Sp(6,R)_R$ irreducible representations in the present approach one needs to involve an $Sp(6,R)_R$ symmetry breaking interaction into the model Hamiltonian.

Finally, in Figure 3, we give the $SU_R(3)$ decomposition of the wave functions for the cluster-model states of the $K^\pi = 0_1^+$, $K^\pi = 0_2^+$, and $K^\pi = 0_1^-$ bands in ^{20}Ne for different angular momentum values. From the figure, we see a similar simple structure for the cluster states of the $K^\pi = 0_1^+$ and $K^\pi = 0_1^-$ bands with a predominant contribution of the $0\hbar\omega/1\hbar\omega$ $SU_R(3)$ multiplet $(8,0)/(9,0)$ and some admixtures due to the mixing to the excited cluster $SU(3)$ configurations. For the $K^\pi = 0_2^+$ band, the predominant contribution is from the $SU_R(3)$ multiplet $(10,0)$ with some small admixtures too. For the ground and $K^\pi = 0_1^-$ bands we have almost a pure ($\sim 99\%$) $SU(3)$ structure, while for the $K^\pi = 0_2^+$ band the admixtures are up to $\sim 4-5\%$. From the figure one sees that for the low-values of the angular momentum (up to $L = 4$) the $SU_R(3)$ amplitudes are approximately L-independent for the states of the three cluster bands under consideration in ^{20}Ne. The latter indicates the presence of a

new type of symmetry, referred to as a quasi-dynamical symmetry in the sense of Refs. [39,40]. Hence, despite of the mixing of the $SU_R(3)$ cluster-model basis states, the microscopic structure of the experimentally observed cluster states of the three bands under consideration shows the presence of an approximate $SU_R(3)$ quasi-dynamical symmetry.

4 Conclusions

In the present work we apply the symplectic symmetry approach to clustering (SSAC) with the essential group structure $Sp(6,R)_R \otimes Sp(6,R)_C \otimes O(A-2) \subset Sp(6(A-1),R)$ to the microscopic description of the lowest $K^\pi = 0_1^+$, $K^\pi = 0_1^-$, and $K^\pi = 0_2^+$ rotational bands in the classical two-cluster $\alpha + {}^{16}\mathrm{O} \rightarrow {}^{20}\mathrm{Ne}$ nuclear system. The latter consist of two scalar $SU(3)$ clusters, so in this particular case the more complete cluster dynamics within the SSAC is reduced to a pure intercluster dynamics of the R-subsystem only. A good description for the excitation energies of these three bands, as well as for the experimentally known $B(E2)$ transition probabilities between the states of the ground band without the use of an effective charge, is obtained. The observed ground-band intraband $B(E2)$ quadrupole dynamics is almost captured by the symplectic bandhead structure of the relevant $Sp(6,R)_R$ irreducible cluster subspace of the nuclear Hilbert space, so a very small vertical mixing is required to slightly enhance the theoretical $B(E2)$ transition strengths to reach the experimental values. Mixed $SU(3)$ irreducible representations are the so-called stretched $SU(3)$ states associated with the relative-motion cluster excitations. Practically a pure $SU(3)$ structure ($\sim 99\%$) is obtained for the ground and and $K^\pi = 0_1^-$ bands, while for the $K^\pi = 0_2^+$ band the admixtures are up to $\sim 4-5\%$.

The interband transition probabilities $B(E2; 0_2^+ \rightarrow 2_1^+)$ and $B(E2; 4_2^+ \rightarrow 2_1^+)$ are, however, significantly underestimated by the theory. The nucleus ^{20}Ne actually represents a complicated structure, which is not easy to be fitted. In Ref. [32] it has been demonstrated to lie very close to the critical point of the quantum phase transition between the $SU(3)$ and $O(6)$ shell-model limits of the ds major shell. The complicated structure of ^{20}Ne suggests to perform more sophisticated SSAC calculations in which both the vertical and horizontal mixings of different $SU(3)$ irreducible representations are involved, in a manner similar to that given in Ref. [38] within a microscopic shell-model version of the Bohr-Mottelson collective model.

References

[1] K. Wildermuth, Y.C. Tang, *A Unified Theory of the Nucleus* (Academic Press, New York, 1977).

[2] W. Greiner, J.Y. Park, W. Scheid, *Nuclear Molecules* (World Scientific, Singapore, 1995).

[3] C. Beck (Ed.) *Clusters in Nuclei*, Vol. 1, Lecture Notes in Physics **818** (Springer-Verlag, Berlin Heidelberg, 2010).

[4] Clusters in Nuclei, Vol. 2, Lecture Notes in Physics **848** (Springer-Verlag, Berlin Heidelberg, 2012).
[5] L.R. Hafstad, E. Teller, *Phys. Rev.* **54** (1938) 681.
[6] M. Freer, *Rep. Prog. Phys.* **70** (2007) 2149.
[7] H. Horiuchi, *J. Phys. G: Nucl. Part. Phys.* **37** (2010) 064021.
[8] M. Freer et al., *Rev. Mod. Phys.* **90** (2018) 035004.
[9] Y. Kanada-En'yo, H. Horiuchi, *Front. Phys.* **13** (2018) 132108.
[10] J.R.M. Berriel-Aguayo, P.O. Hess, *Symmetry* **12** (2020) 738.
[11] A. Bohm, Y. Ne'eman, A.O. Barut et al., *Dynamical Groups and Spectrum Generating Algebras* (World Scientific, Singapore, 1988).
[12] R. Bijker, F. Iachello, *Phys. Rev. Lett.* **112** (2014) 152501.
[13] D.J. Marin-Lambarri et al., *Phys. Rev. Lett.* **113** (2014) 012502.
[14] R. Bijker, F. Iachello, *Phys. Rev. Lett.* **122** (2019) 162501.
[15] R. Bijker, F. Iachello, *Prog. Part. Nucl. Phys.* **110** (2020) 103735.
[16] F. Iachello, A.D. Jackson, *Phys. Lett.* **B108** (1982) 151.
[17] F. Iachello, *Nucl. Phys. A* **396** (1983) 233c.
[18] H. Daley, F. Iachello, *Phys. Lett. B* **131** (1983) 281.
[19] H.J. Daley, F. Iachello, *Ann. Phys.* **167** (1986) 73.
[20] H. Daley, B. Barrett, *Nucl. Phys. A* **449** (1986) 256.
[21] J. Cseh, *Phys. Lett. B* **281** (1992) 173.
[22] J. Cseh, G. Levai, *Ann. Phys. (N.Y.)* **230** (1994) 165.
[23] J. Cseh, *Phys. Lett. B* **743** (2015) 213.
[24] H.G. Ganev, *Commun. Theor. Phys.* **77** (2025) 055301.
[25] H.G. Ganev, *Nucl. Phys. A* **1062** (2025) 123162.
[26] M. Harvey, In: *Advances in Nuclear Physics*, Vol. 1, edited by M. Baranger, E. Vogt (Plenum Press, New York, 1968).
[27] Y. Akiyama, A. Arima, T. Sebe, *Nucl. Phys. A* **138** (1969) 273.
[28] G. Rosensteel, D.J. Rowe, *Ann. Phys.* **126** (1980) 343.
[29] J. Escher, A. Leviatan, *Phys. Rev. C* **65** (2002) 054309.
[30] D.J. Rowe, *Rep. Prog. Phys.* **48** (1985) 1419.
[31] T. Dytrych et al., *Phys. Rev. Lett.* **124** (2020) 042501.
[32] G. Rosensteel, D. Rowe, *Nucl. Phys. A* **797** (2007) 94.
[33] V.V. Vanagas, *Algebraic Methods in Nuclear Theory* (Mintis, Vilnius, 1971) (in Russian).
[34] P. von Brentano, N.V. Zamfir, R.F. Casten, W.G. Rellergert, E.A. McCutchan, *Phys. Rev. C* **69** (2004) 044314.
[35] S. Frauendorf, *Int. J. Mod. Phys. E* **24** (2015) 1541001.
[36] H.G. Ganev, *Chin. Phys. C* **48** (2024) 014102.
[37] National Nuclear Data Center (NNDC), http://www.nndc.bnl.gov/.
[38] H.G. Ganev, *Chin. Phys. C* **46** (2022) 044105.
[39] C. Bahri, D. Rowe, *Nucl. Phys. A* **662** (2000) 125.
[40] D.J. Rowe, In: *Computational and Group-Theoretical Methods in Nuclear Physics*, edited by J. Escher, O. Castanos, J. Hirsch, S. Pittel, G. Stoitcheva (World Scientific, Singapore, 2004), pp. 165-173.